doi:10.1016/j.jmb.2010.10.027 J. Mol. Biol. (2011) 405, 254–273

Contents lists available at www.sciencedirect.com

Journal of Molecular Biology

journal homepage: http://ees.elsevier.com.jmb

The Anti-Parkinsonian Drug Selegiline Delays the Nucleation Phase of α-Synuclein Aggregation Leading to the Formation of Nontoxic Species

Carolina A. Braga[1]†, Cristian Follmer[1]†, Fernando L. Palhano[1], Elias Khattar[1], Mônica S. Freitas[1], Luciana Romão[2], Saviana Di Giovanni[3], Hilal A. Lashuel[3], Jerson L. Silva[1] and Debora Foguel[1]*

[1]*Programa de Biologia Estrutural, Instituto de Bioquímica Médica, Centro de Ciências da Saúde, Universidade Federal do Rio de Janeiro, Rio de Janeiro, RJ 21941-590, Brazil*
[2]*Instituto de Ciências Biomédicas, Departamento de Anatomia, Universidade Federal do Rio de Janeiro-Macaé, Macaé, RJ, Brazil*
[3]*Laboratory of Molecular Neurobiology and Neuroproteomics, Brain Mind Institute, Ecole Polytechnique Federale de Lausanne, CH-1015 Lausanne, Switzerland*

Received 8 April 2010; received in revised form 28 August 2010; accepted 16 October 2010
Available online 2 November 2010

Edited by S. Radford

Keywords:
selegiline;
dopamine;
Parkinson's disease;
α-synuclein;
aggregates toxicity

Parkinson's disease (PD) is a movement disorder characterized by the loss of dopaminergic neurons in the substantia nigra and the formation of intraneuronal inclusions called Lewy bodies, which are composed mainly of α-synuclein (α-syn). Selegiline (Sel) is a noncompetitive monoamino oxidase B inhibitor that has neuroprotective effects and has been administered to PD patients as monotherapy or in combination with L-dopa. Besides its known effect of increasing the level of dopamine (DA) by monoamino oxidase B inhibition, Sel induces other effects that contribute to its action against PD. We evaluated the effects of Sel on the *in vitro* aggregation of A30P and wild-type α-syn. Sel delays fibril formation by extending the lag phase of aggregation. In the presence of Sel, electron microscopy reveals amorphous heterogeneous aggregates, including large annular species, which are innocuous to a primary culture enriched in dopaminergic neurons, while their age-matched counterparts are toxic. The inhibitory effect displayed by Sel is abolished when seeds (small fibril pieces) are added to the aggregation reaction, reinforcing the hypothesis that Sel interferes with early nuclei formation and, to a lesser extent, with fibril elongation. NMR experiments indicate that Sel does not interact with monomeric α-syn. Interestingly, when added in combination with DA (which favors the formation of toxic protofibrils), Sel overrides the

*Corresponding author. E-mail address: foguel@bioqmed.ufrj.br.
† C.A.B. and C.F. contributed equally to this work.
Present address: C. Follmer, Instituto de Química, Departamento de Físico-Química, Universidade Federal do Rio de Janeiro, Rio de Janeiro, RJ, Brazil.

Abbreviations used: PD, Parkinson's disease; α-syn, α-synuclein; Sel, selegiline; DA, dopamine; MAO-B, monoamino oxidase B; MPTP, 1-methyl-4-phenyl-1,2,3,6-tetrahydropyridine; ROS, reactive oxygen species; DA, dopamine; WT, wild type; Thio-T, thioflavin T; TTR, transthyretin; EM, electron microscopy; HSQC, heteronuclear single quantum coherence; A30P-F, preformed A30P fibrils; LS, light scattering; DAPI, 4′, 6-diamidino-2-phenylindole; EGCG, epigallocatechin gallate; PBS, phosphate-buffered saline.

inhibitory effect of DA and favors fibrillation. Additionally, Sel blocks the formation of smaller toxic aggregates by perturbing DA-dependent fibril disaggregation. These effects might be beneficial for PD patients, since the sequestration of protofibrils into fibrils or the inhibition of fibril dissociation could alleviate the toxic effects of protofibrils on dopaminergic neurons. In nondopaminergic neurons, Sel might slow the fibrillation, giving rise to the formation of large nontoxic aggregates.

Introduction

The pathological characteristics of Parkinson's disease (PD) include the preferential loss of dopaminergic neurons in the substantia nigra and the formation of intraneuronal fibrillar inclusions called Lewy bodies, which are composed mainly of α-synuclein (α-syn).[1–4] Although the precise mechanism underlying this selective cell loss has not yet been elucidated, α-syn aggregation is an invariant feature of the sporadic and familial forms of PD and has been observed in the pathogenesis of multiple system atrophy and dementia with Lewy bodies. These and other neurodegenerative disorders characterized by α-syn inclusions are collectively known as synucleinopathies.[5] Furthermore, a central role of α-syn in the pathogenesis of PD is supported by strong genetic evidence:[6–10] (1) three missense mutations in α-syn (A30P, A53T, and E46K) are associated with autosomal-dominant inherited forms of PD; (2) duplication and triplication in a region that encompasses the α-syn gene on chromosome 4 are sufficient to cause familial PD; and (3) all familial PD mutations accelerated the aggregation of α-syn *in vitro*, but not necessarily fibrillation.[7,11–13]

Selegiline (Sel; *R*(−)-deprenyl) (Fig. 1a) is a noncompetitive irreversible monoamino oxidase B (MAO-B) inhibitor that was first synthesized as a "psychic energizer."[14] The neuroprotective activity of Sel became evident when it was found to be able to block the effect of 1-methyl-4-phenyl-1,2,3,6-tetrahydropyridine (MPTP), a neurotoxin that induces pathological abnormalities similar to those observed in PD patients.[15–17] MPTP is oxidized to MPP^{+-} (the active form of the toxin) by MAO-B in glial cells and is taken up by dopaminergic neurons, where it leads to neuronal death by generating reactive oxygen species (ROS) and by interfering with mitochondria respiration and other cellular processes.[18,19] It is possible that there is an endogenous toxin that mimics MPP^+, leading to oxidative stress in dopaminergic neurons and ultimately to idiopathic PD. Additionally, tyrosine hydroxylase [involved in dopamine (DA) biosynthesis] and monoamino oxidase (involved in DA breakdown) both generate ROS (H_2O_2) as a result of their role in DA (Fig. 1a) metabolism. Thus, inhibition of MAO-B seems to be an attractive strategy for quelling PD symptoms and inhibiting disease progression, since the net effect is a decrease in the concentration of ROS and an increase in the concentration of DA.

Sel has been administered to patients in the early stage of PD either as monotherapy or in combination with L-dopa.[20] In the former, Sel treatment leads to a mild anti-parkinsonian effect, thus delaying the need for L-dopa therapy in these patients. When combined with L-dopa, Sel potentiates the effects of L-dopa, allowing for a reduction in its daily dose, which is a benefit given its adverse side effects.[21,22] Mytilineou et al.[23] reported that aside from preventing free radical formation through MAO-B inhibition, Sel also exerts neuroprotection by increasing the anti-oxidant defenses of the cells through stimulation of the synthesis of neurotrophic factors and by modulating the apoptotic pathway.[24,25] Some of these effects are independent of MAO-B inhibition, since they occur in concentrations below those required to inhibit MAO-B. However, until now, the precise mechanism and site of action of Sel have remained uncertain. The doses of Sel used in the treatment of patients with parkinsonism range from 1.25 to 10 mg/day.[20,26]

Recently, Ono et al. demonstrated the inhibitory effect of Sel and other anti-parkinsonian agents on the *in vitro* aggregation of wild-type (WT) α-syn.[27] They also demonstrated the disaggregating properties of Sel on preformed α-syn fibrils. In the present study, we investigated the effects of Sel alone or in combination with DA on the *in vitro* aggregation of A30P and WT α-syn. The purposes of the study were to provide more insights into the mechanism of action of Sel, to more closely simulate the scenario of PD when these two compounds are administered together as therapeutic agents, and to elucidate the potential of Sel as an anti-fibrillogenic agent in familial PD.

Our data show that Sel (α-syn/Sel molar ratio $\geq$1:0.5) inhibits the fibrillation of A30P and WT α-syn by delaying the nucleation phase. By utilizing bidimensional NMR, we were able to show that Sel does not interact with any specific amino acid residue in soluble α-syn. Experiments in primary cultures of dopaminergic neurons demonstrated that aggregates formed in the presence of Sel in the nucleation phase are innocuous, while age-matched aggregates cause cell death. Furthermore, the combination of DA Sel

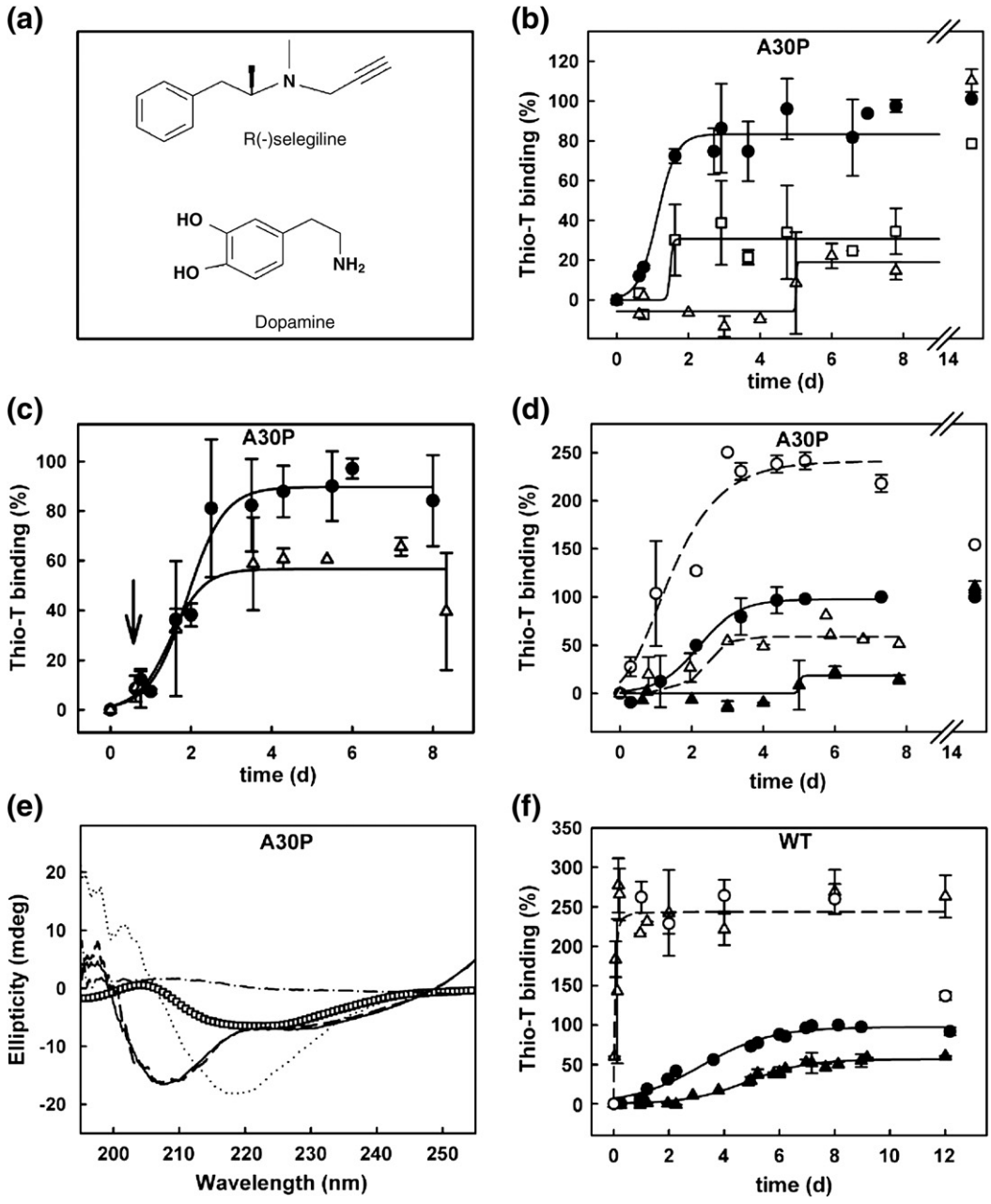

Fig. 1. Effect of Sel on α-syn fibril formation. (a) Structures of Sel (*R*(−)-deprenyl) and DA. (b) A30P (140 μM) was incubated at 37 °C, with stirring (185 rpm), in the absence (filled circles) or in the presence of 70 μM Sel (hollow squares) or 200 μM Sel (hollow triangles) for 15 days. Fibril formation was monitored by Thio-T binding. (c) A30P (140 μM) was incubated under aggregating conditions. After 15 h, 200 μM Sel was added to one-half of this solution (arrow, hollow triangles), and Thio-T binding was evaluated over time. An equivalent volume of buffer was added to the control sample (filled circles). (d) Effect of Sel on the nucleation phase of A30P aggregation. A30P (140 μM) was stirred in the absence (filled circles) or in the presence (hollow circles) of 5% seeds at 37 °C. The aggregation of A30P in the presence of 200 μM Sel is shown as filled triangles, while the aggregation of A30P in the presence of 200 μM Sel and 5% seeds is shown as hollow triangles. Aggregation kinetics was monitored by Thio-T binding. (e) CD spectra of 140 μM A30P in solution (full line) or incubated for 4 days under aggregating conditions in the absence (dotted lines) or in the presence (hollow squares) of 200 μM Sel. A long broken line shows the spectrum of soluble A30P Sel (overlapped with the spectrum of soluble A30P) and the spectrum of Sel alone (dot/dash line). (f) WT α-syn (140 μM) was incubated under aggregating conditions for 12 days in the absence (filled circles) or in the presence (filled triangles) of 200 μM Sel. Hollow circles show the aggregation of WT protein in the presence of 5% seeds, while hollow triangles show aggregation in the presence of 200 μM Sel and 5% preformed WT seeds.

leads to the appearance of amyloid fibrils, suggesting that Sel counteracts the inhibitory effect of DA on fibril formation. These data provide new insights into the mechanisms underlying the *in vivo* effects of Sel and suggest that Sel decreases the concentration of neurotoxic protofibrils by increasing fibril formation, even in the presence of DA. Such an effect, in addition to Sel-mediated MAO-B inhibition, could be beneficial to PD patients.

Results

Effects of Sel on the *in vitro* aggregation kinetics of α-syn

In vitro, α-syn exists as an ensemble of disordered structures.[28] In the absence of mechanical agitation or other additives, α-syn fibrillization is a very slow process that requires incubation for weeks even at 37 °C.[29,30] Interestingly, overexpression of α-syn in cellular models of synucleinopathies is not sufficient to drive its fibrillization in the absence of external stimuli (i.e., exposure to free radicals and metals; e.g., Fe^3).[31] Therefore, to investigate the aggregation properties of α-syn *in vitro* in a feasible timescale, we used micromolar concentrations of protein.[32–34] This implies the use of Sel in the same concentration range to keep the molar ratio close to 1, although it is physiologically reasonable to assume that nanomolar concentrations of Sel penetrate the intracellular milieu when administered to PD patients. As a result of these limitations, all our aggregation studies were carried out at the micromolar concentrations of both molecules. Initially, we evaluated the effects of 17 and 35 μM Sel on the aggregation of 140 μM A30P α-syn (α-syn/Sel ratios close to 1:0.1 and 1:0.2; Supplementary Fig. 1a). At these substoichiometric ratios, we did not observe a considerable effect of Sel on the aggregation of α-syn after 48 or 72 h. The same results were observed for WT α-syn (Supplementary Fig. 1b; see the bar related to a α-syn/Sel ratio of 1:0.1). Thus, all further experiments were performed using ratios of 1:0.5 (α-syn/Sel)—the lowest molar ratio at which Sel was stated to be effective in inhibiting α-syn aggregation (Supplementary Fig. 1).

Given the previous reports of Ono *et al.* on the effect of Sel on the aggregation of WT α-syn,[27] we decided to focus on the disease-associated mutant A30P and to compare it to the WT protein when the effect of Sel on A30P appears to differ from previously reported results on WT α-syn. This specific variant was chosen in a first approach since it accelerates the events in the oligomerization process of α-syn and attenuates the helical propensity found in the N-terminal region of the protein previously observed by NMR experiments—features that were not observed with A53T.[7,35]

In order to evaluate if Sel would interfere with the aggregation kinetics of A30P as it did with the aggregation of the WT protein,[27] we incubated 140 μM A30P in the absence (Fig. 1b, circles) or in the presence of 70 μM Sel (squares) or 200 μM Sel (triangles) under aggregating conditions. Thioflavin T (Thio-T) binding (Fig. 1b) and turbidity (absorbance at 330 nm; data not shown) were measured periodically during 15 days of incubation. In the absence of Sel, the aggregation of A30P displayed a nucleation-dependent polymerization profile[34,36] with a short lag phase of ~18 ± 3 h in which no change in Thio-T binding (Fig. 1b) or no absorbance at 330 nm (data not shown) was detected. This result is consistent with previously published studies.[12,37] It has been shown that in the lag phase, small oligomers, which act as the seeds or nuclei of the aggregation reaction, are formed.[34,36] After this period, fibril growth occurs in a cooperative manner, resulting in a large increase in Thio-T binding and in absorbance at 330 nm. In the presence of 70 or 200 μM Sel (α-syn/Sel molar ratio of 1:0.5 or 1:1.5), nuclei formation was drastically delayed (Fig. 1b, squares and triangles, respectively), and the lag phase was extended to approximately 1.5 and 5 days, respectively. Besides, after 6–8 days under aggregating conditions, fibrillation almost leveled off in the control sample, while it was inhibited by ~70–80% in the presence of 70 and 200 μM Sel, suggesting that Sel also has some effect on fibril growth inhibition. However, after 15 days of aggregation in the presence of Sel, the amounts of fibrils formed in the absence and in the presence of Sel attained equal amounts (see isolated symbols on the right of Fig. 1b). Altogether, these results suggest that Sel inhibits the aggregation of A30P as well as it inhibits the aggregation of the WT protein,[27] but its effect seems to be more specific for nuclei formation, thus extending the lag phase of A30P aggregation.

In order to explore more carefully the effect of Sel on nuclei formation, we incubated 140 μM A30P under aggregating conditions for 18 h until the nuclei had formed. At this point, 200 μM Sel was added to the solution (Fig. 1c, arrow, triangles). Despite the excess amounts of Sel, it was not able to extend the lag phase under these conditions; after 8 days of aggregation, Thio-T binding had only slightly diminished in the sample containing Sel. This result reinforces the idea that Sel exerts its activity more prominently on the initial phase of fibril formation (i.e., the nucleation phase).

Additional evidence of the effect of Sel on the nucleation phase of A30P aggregation comes from the experiments described in Fig. 1d. As previously shown,[36,37] addition of preformed seeds (prepared by the fragmentation of mature fibrils by sonication) accelerates the fibrillation process by abolishing the nucleation phase. Figure 1d shows that the addition of seeds (5%) to an aggregating solution of A30P abolished the lag phase (compare the seeded curve

in hollow circles and broken line with the unseeded curve in filled circles and continuous line). Again, addition of Sel in a molar ratio of 1:1.5 extended the nucleation phase to 5 days (filled triangles and continuous line). Nevertheless, when fibrillation was performed in the presence of Sel (1:1.5) and 5% seeds (hollow triangles and broken line), the inhibitory effect of Sel on the nucleation of A30P was drastically reduced, reinforcing the idea that the major effect of Sel is on nuclei formation. Note again that after 15 days, both seeded reactions (control and Sel) attained equivalent Thio-T binding levels, consistent with the idea that Sel has little effect on the growth phase of A30P aggregation once nuclei are formed.

Previous studies indicate that β-sheet formation is a crucial early step in the amyloidogenesis of α-syn[38,39] and is a signature of amyloid fibril formation. To evaluate the effects of Sel on β-sheet formation, we performed circular dichroism (CD) measurements (Fig. 1e). Since α-syn is unfolded in its native state, its CD spectrum has no minimum in the range 210–230 nm, where α-helices and β-sheets absorb. Instead, it displays a negative minimum at around 200–205 nm (Fig. 1e, continuous line), indicative of disorganized random coils (calculated as 58% of random coils). The CD spectrum of A30P fibrils formed after 4 days under aggregating conditions displayed a decreased negativity at 205 nm and an increased minimum at ~220 nm, characteristic of β-sheets present in the amyloid fold (Fig. 1e, dotted line; calculated as 58% β-sheets and 5.5% random coils).[40] However, the spectrum of the sample incubated for 4 days in the presence of Sel (200 μM) displayed a less intense signal at 220 nm, consistent with the presence of fewer β-sheet-rich structures in these samples. Furthermore, the random-coil signal also diminished, consistent with the conversion of soluble unfolded α-syn into a more ordered species (Fig. 1e, open squares; calculated as 40% β-sheets). Figure 1e also presents the CD spectrum of Sel alone (dot/dash line) and the spectrum of soluble A30P in the presence of 200 μM Sel (long broken line), which is superimposed on that displayed by soluble A30P. These results suggest that the presence of Sel does not compromise or induce any structural alteration on α-syn secondary structure.

To assess if the inhibitory effect of Sel was specific for α-syn, we evaluated Sel activity against the yeast prion Sup35, which is also natively unfolded, and transthyretin (TTR), which is an amyloidogenic β-sheet-rich homotetrameric protein. A 4-fold molar excess of Sel (Supplementary Fig. 2, long broken line) drastically inhibited the aggregation of Sup35 by delaying the nucleation phase and by decreasing the total amount of fibrils at the end of the fibrillation process. In this case, however, Sel activity was not abolished when it was added at the end of the lag phase (18 min, arrow), suggesting that Sel also blocks the growth process of Sup35 fibrillation (Supplementary Fig. 2, dotted line). In contrast, Sel was incapable of inhibiting TTR aggregation at a TTR/Sel molar ratio of 1:1 or 1:4 (data not shown). As previously shown, aggregation of TTR is initiated from a partially unfolded monomer, which aggregates without a lag phase.[41] It is possible that the lack of a defined and/or stable nucleus in the aggregation of TTR explains the inefficacy of Sel as an inhibitor.

Ono et al. had already described the inhibitory effect of Sel on the *in vitro* aggregation of WT α-syn.[27] However, its precise mechanism of action was not explored in that study. In order to evaluate whether Sel exerts its effect on WT aggregation by interfering with nuclei formation, we performed the same experiment presented in Fig. 1d (Sel seed addition), but with the WT protein. As shown in Fig. 1f, addition of 200 μM Sel inhibited the aggregation of WT α-syn by ~50% and extended the nucleation phase from 18 h (filled circles) to ~3 days (filled triangles). As expected, addition of 5% seeds drastically accelerated the aggregation of WT α-syn, abolishing the lag phase (hollow circles). However, when 200 μM Sel was added to a seeded aggregation reaction (hollow triangles), its inhibitory effect was abolished, thus confirming that Sel interferes more prominently with nuclei formation in both WT and A30P α-syn aggregation. It seems clear from the experiments described in Fig. 1d (A30P) and Fig. 1f (WT) that seed addition was much more effective in reverting the effect of Sel in the latter case. The precise explanation for this observation is not known at the present moment, but one has to take into account that the substitution at position 30 changes the important features of the A30P aggregation reaction, such as an increased tendency to oligomerize.[12]

Morphology of aggregates formed in the presence of Sel

In order to compare the morphology of the aggregates formed in the presence of Sel and the morphology of the aggregates formed in the absence of Sel, we examined the samples by negative-staining transmission electron microscopy (EM) (Fig. 2). In Fig. 2a, we show the aggregates formed by A30P (140 μM) in the absence of 200 μM Sel (−Sel; left) or in the presence of 200 μM Sel (Sel; right). After 15 h under aggregating conditions in the absence of Sel (Fig. 2a, upper left), most of the fields displayed amorphous and annular aggregates with no detectable fibrillar structures. Most of the annular species possess diameters of approximately 15–20 nm (arrows on the upper left), similar to the oligomers previously observed for this variant.[32] Another population of amorphous aggregates was also observed (dispersed all over the grid and shown by an arrowhead). In the

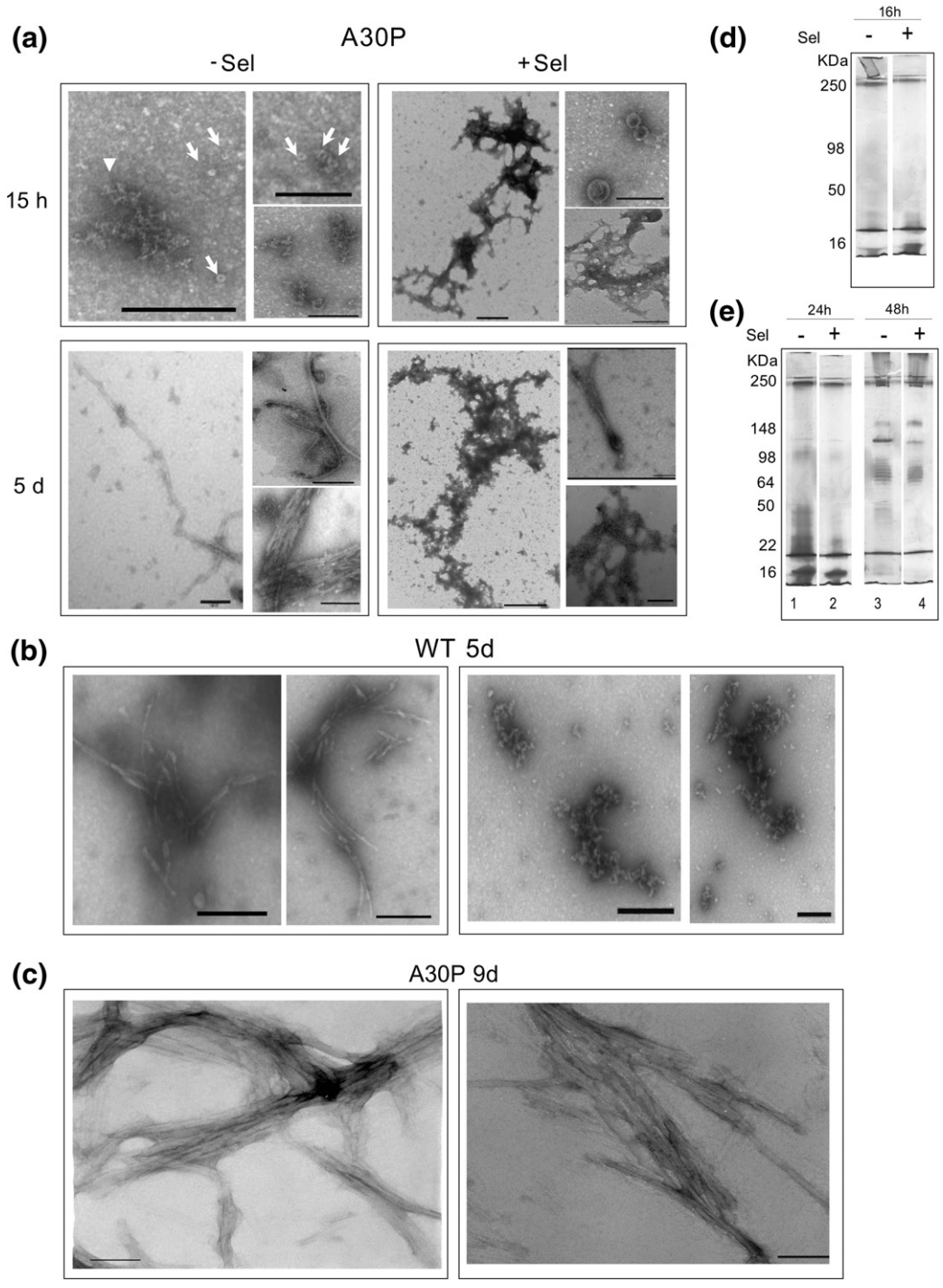

Fig. 2. Morphology of the aggregates formed in the absence (−Sel) or in the presence (Sel) of 200 μM Sel. (a) A30P aggregates formed after 15 h or 5 days under aggregating conditions. (b) Five-day-old WT aggregates. (c) Nine-day-old A30P fibrils. In (a)–(c), the left images show the aggregates grown in the absence of Sel, while the right images show those formed in its presence. Bars correspond to 0.2 μm. (d) A 15% SDS-PAGE of the 16-h-old aggregates of A30P (140 μM) grown in the absence (−) or in the presence () of 200 μM Sel. (e) Same as in (d), but the aggregates here are 24 h old (lanes 1 and 2) or 48 h old (lanes 3 and 4). SeeBlue® Plus2 Pre-Stained Standard was used as molecular weight standard.

sample incubated in the presence of Sel (200 μM), amorphous coalescent aggregates were observed after 15 h under aggregating conditions (Fig. 2a, upper right). We also detected in the latter sample large annular aggregates with a diameter ranging from 40 to 100 nm (Fig. 2a, upper right). These annular

structures seem to be aberrant in size and diameter compared to those typically observed during α-syn aggregation, which are shown on the images on the left side of Fig. 2a. After 5 days under aggregating conditions, the control sample exhibited mostly fibrillar assemblies (Fig. 2a, lower left); however, in the sample incubated in the presence of 200 μM Sel, amorphous aggregates predominated, with some fibrils being observable (lower right).

The morphology of the aggregates formed from WT α-syn was also analyzed by EM (Fig. 2b). After 5 days under aggregating conditions, we observed mostly fibers in the control sample (left), while the aggregates formed in the presence of Sel were predominantly heterogeneous and amorphous (right).

The data presented in Fig. 1b show that after long incubation times under aggregation conditions in the absence or in the presence of Sel, the same amount of Thio-T-binding-competent species is formed. The EM images of Fig. 2c show that, indeed, after 9 days under aggregating conditions, there are large amounts of mature amyloid fibrils in the sample incubated in the absence (left) or in the presence (right) of 200 μM Sel.

Taken together, the EM analyses reinforce the idea that Sel delays the aggregation of A30P and WT α-syn most likely by inhibiting the formation of on-pathway aggregates that constitute the nuclei for the aggregation reaction. In the presence of Sel, large amorphous coalescent aggregates or large annular species are found, and these species retard the formation of mature fibers, although the extent of fibril formation or the Thio-T-positive species are comparable to the control sample at long incubation times.

Aiming to better characterize the prefibrillar aggregates formed by α-syn in the absence or in the presence of Sel, we analyzed their resistance to SDS. As previously shown, the early aggregates formed during WT α-syn fibrillogenesis are soluble and susceptible to the conversion into monomers by SDS. On the contrary, the late formed aggregates and the mature fibrils precipitate but are solubilized into a myriad of oligomers with high molecular weights.[42] Figure 2d shows the migration profiles of the aggregates formed in the absence (left lane) or in the presence (right lane) of 200 μM Sel after 16 h of aggregation. Note that they responded similarly to SDS treatment, with all of them being susceptible to the detergent. However, after 24 h of aggregation in the absence of Sel, it is possible to detect some aggregates that are SDS resistant (Fig. 2e, lane 1). Interestingly, in the presence of Sel, at this time point, only a few SDS-resistant aggregates are present (Fig. 2e, lane 2), probably because Sel delays the maturation of these aggregates. After 48 h of aggregation, SDS-resistant aggregates are present under both conditions (Fig. 2e, lanes 3 and 4). As previously shown, the aggregates formed in the presence of DA were shown to be SDS resistant since the beginning of the aggregation reaction.[42,43] Thus, we can conclude that the aggregates formed in the presence of Sel, despite their aberrant morphology (Fig. 2a), respond to SDS as their counterparts grown in the absence of Sel.

Effect of DA and Sel on A30P aggregation

Since Sel has been administered to PD patients in combination with L-dopa,[20,22] which is converted into DA (Fig. 1a) by dopaminergic neurons, we evaluated the combined effect of Sel and DA on the aggregation process of A30P. Figure 3 shows Thio-T binding to A30P (140 μM) incubated in the absence (filled circles) or in the presence of DA (1:1 A30P/DA) and DA Sel (1:1:1.5 A30P/DA/Sel). As has been demonstrated previously and as has been confirmed in the curve in hollow circles, DA inhibits the fibrillation process of α-syn, leading to the accumulation of protofibrils.[44,45] However, the presence of Sel partially counteracted this inhibitory effect of DA, leading to the appearance of species that bind Thio-T (hollow triangles). These data are better visualized in Fig. 3b, where aggregation in the absence of any additive was construed as 100%. DA inhibits 87% of fibril formation, while DA Sel inhibit aggregation by ~60%.

Figure 3c shows the morphology of the aggregates of A30P formed in the presence of 140 μM DA after 6 days of incubation under aggregating conditions, where only annular structures with diameters of 20–40 nm were observed. Figure 3d and e show the aggregates of A30P formed in the presence of 140 μM DA 200 μM Sel after 2 and 6 days, respectively. After 2 days under aggregation, some small annular oligomers are observable (Fig. 3d, arrows), while fibrils were observed in the samples after 6 days (Fig. 3e).

This counteracting effect of Sel on DA activity is intriguing, and one possible explanation for it would be that Sel binds directly to DA, leading to coaggregation of the two compounds. Also, Sel could interfere with DA oxidation, abolishing its effect on α-syn aggregation, since an oxidized state of DA responds to its activity, as shown previously.[43] These possibilities do not seem to be the case. Supplementary Figure 3a shows that oxidation of DA, as measured by the increase in absorbance at 386 nm,[46] is slightly retarded in the presence of Sel but achieves equal levels after 3–4 days of incubation at 37 °C. Besides, we can rule out that the two compounds coaggregate in solution because the absorbance at 386 nm of a solution that remained for 10 days at 37 °C after its centrifugation or filtration is equal to that displayed by a solution incubated with these two compounds and not filtered or centrifuged (Supplementary Fig. 3b).

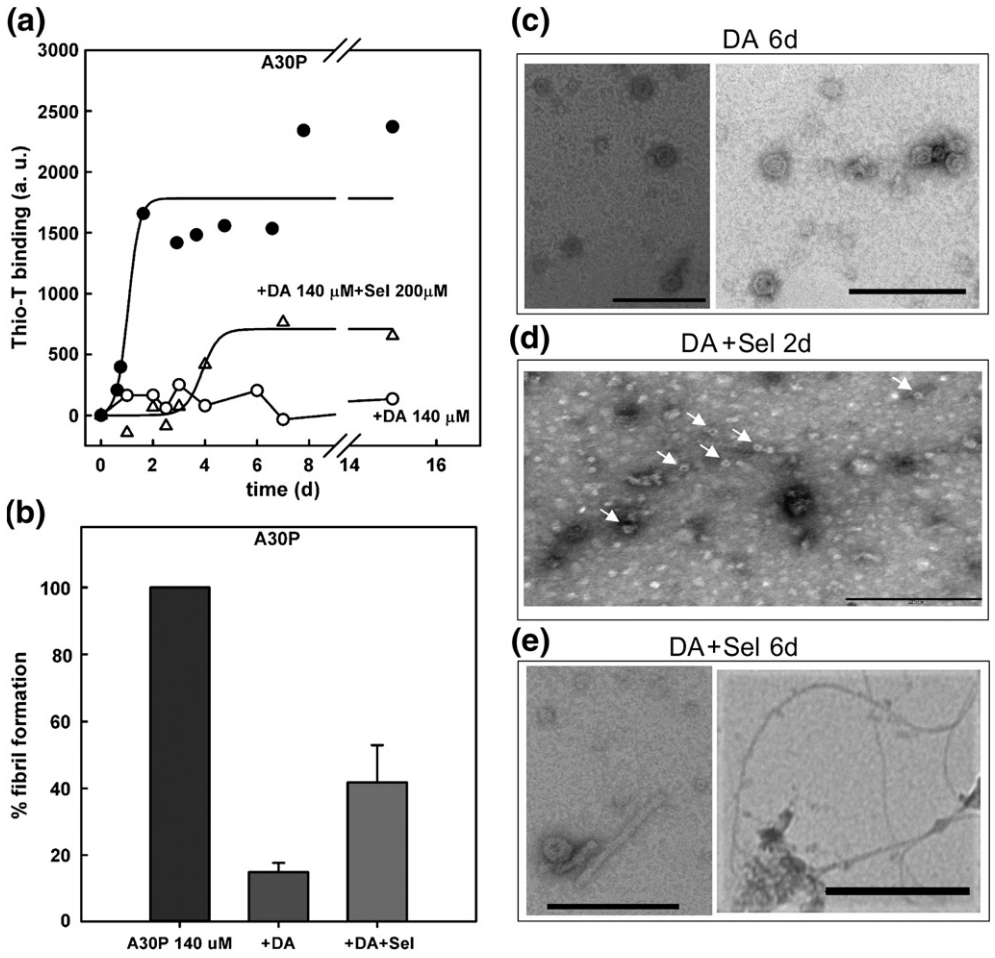

Fig. 3. Effects of DA Sel on A30P fibrillation. (a) A30P (140 μM) was incubated under aggregating conditions for 15 days in the absence of 140 μM DA (filled circles), in the presence of 140 μM DA (hollow circles), or in the presence of DA Sel (140 μM DA 200 μM Sel; hollow triangles). Aggregation was followed by Thio-T binding. (b) Percentage of fibril formation calculated from Thio-T binding after 6 days of incubation. Thio-T binding to A30P alone was normalized to 100%. (c–e) EM images of A30P incubated in the presence of 140 μM DA for 6 days (c), in the presence of 140 μM DA 200 μM Sel for 2 days (d), or in the presence of 140 μM DA 200 μM Sel for 6 days (e). Bars correspond to 0.2 μm.

Taking all these observations together, we can conclude that the counteracting effect of Sel on DA is neither due to the coaggregation of both compounds nor due to the inhibition of the formation of the active oxidation product of DA by Sel.

Sel does not bind to unfolded monomeric α-syn

In order to obtain structural details about α-syn/Sel interaction, we took advantage of NMR spectroscopy to compare the chemical shift deviations induced by Sel binding to map the interacting residue(s) in α-syn. For this purpose, the heteronuclear single quantum coherence (HSQC) spectrum obtained in the absence of Sel (Fig. 4, green spectrum) was overlaid to that obtained in the presence of Sel (purple spectrum). The spectrum of A30P α-syn exhibited a characteristic profile of a natively unfolded protein with limited resonance dispersion in the proton dimension and good dispersion in the nitrogen dimension.[48,49] Upon Sel addition (1:1 A30P/Sel), no significant chemical shift changes were observed (Fig. 4, inset), suggesting that Sel does not bind to monomeric A30P α-syn. Even the addition of Sel at a higher molar ratio (1:5) did not promote any considerable chemical shift deviation (data not shown).

Sel disassembles preformed A30P fibrils

As shown previously by Li *et al.*, DA is able to disassemble preformed α-syn fibrils.[50] In order to probe Sel for its capability to counteract this property of DA, we diluted preformed A30P fibrils (A30P-F) to 10 μM and incubated them at 37 °C in the presence of Sel (10 or 40 μM A30P-F Sel) or

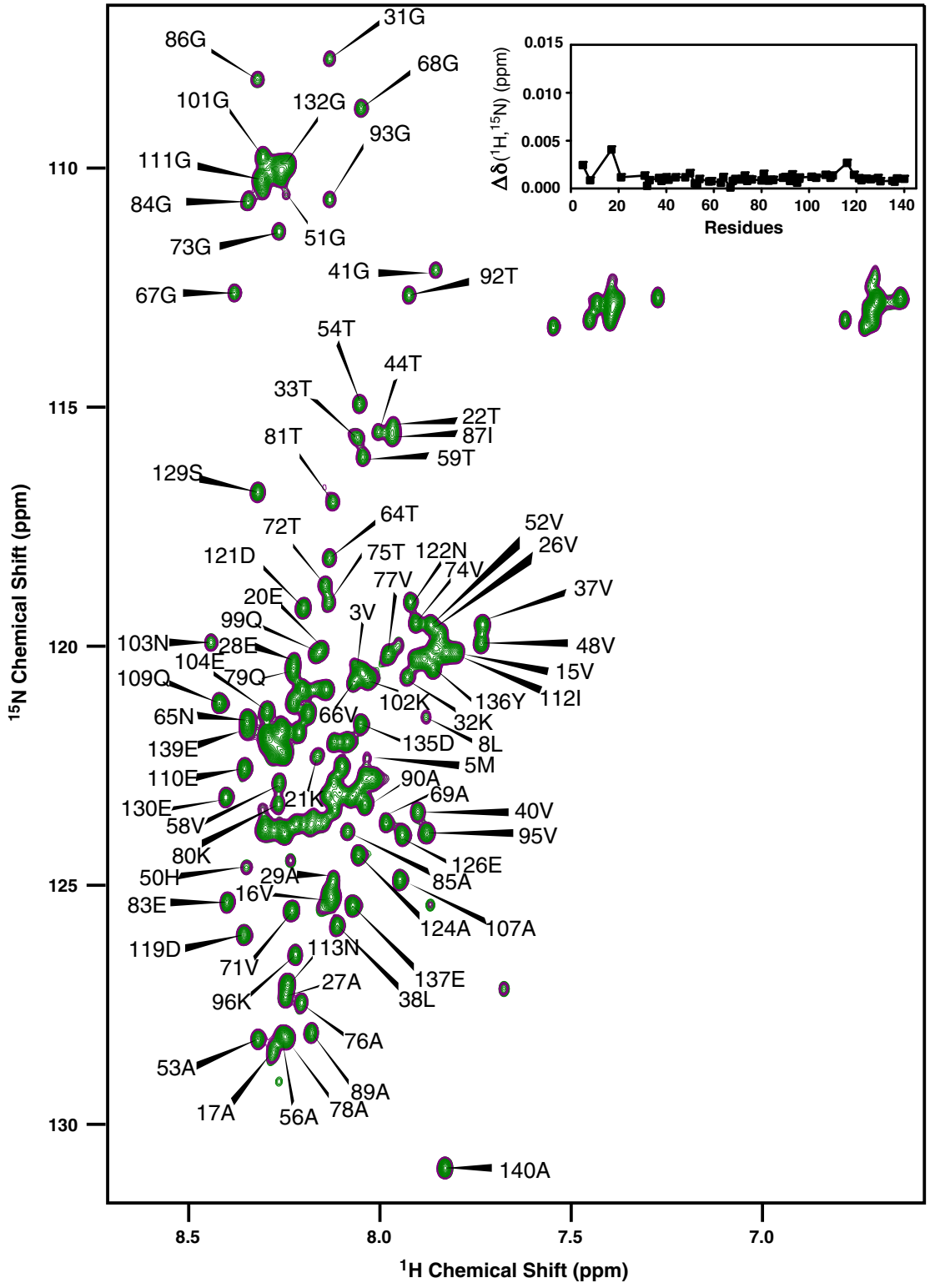

Fig. 4. Mapping α-syn interaction with Sel by NMR. Overlay of the ^{1}H-^{15}N HSQC spectra of A30P (350 μM) in the absence (green spectrum) or in the presence (purple spectrum) of 350 μM Sel. The inset shows chemical shift deviations in ^{1}H-^{15}N HSQC related to α-syn in the presence and in the absence of Sel for the data presented in (a). The average chemical shift changes were calculated as shown by Lendel et al.[47]

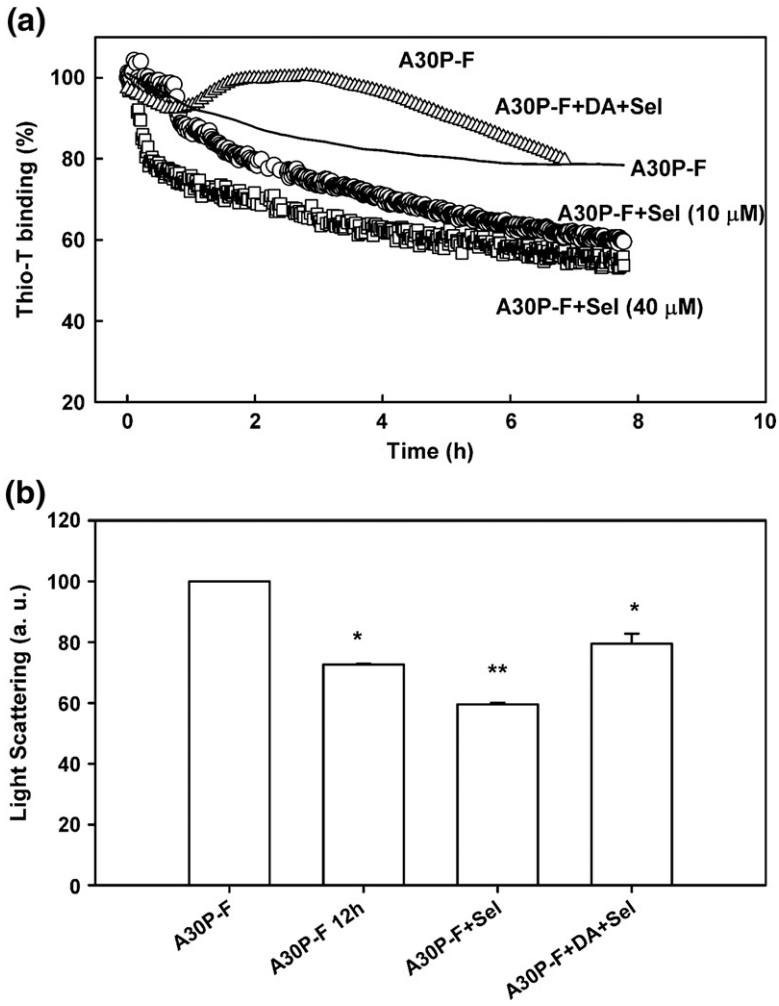

Fig. 5. Sel promotes the disassembly of A30P-F. (a) A30P (140 μM) was incubated at 37 °C, with stirring, for 15 days to produce fibrils. The fibrils were pelleted and diluted to 10 μM in a solution containing 30 μM Thio-T at 37 °C. Destabilization of these fibrils was monitored by changes in Thio-T fluorescence signal in the absence (full line) or in the presence of 10 or 40 μM Sel (circles and squares, respectively) or 40 μM Sel 10 μM DA (triangles). (b) LS values obtained after 12 h of dilution of A30P fibrils in buffer or in the presence of 40 μM Sel or 40 μM Sel 10 μM DA. This experiment was performed in the absence of Thio-T to avoid competition between Thio-T and the other compounds for the same binding site.

both DA and Sel (A30P-F DA Sel) (Fig. 5a). As seen in Fig. 5a, dilution of the fibrils in buffer alone led to an ~20% decrease in Thio-T binding (continuous line) due to the spontaneous dissociation of the α-syn fibrils. This result is confirmed by the decrease in the light scattering (LS) value observed after 12 h of dilution (Fig. 5b). However, when fibrils were diluted in the presence of Sel at an A30P-F Sel ratio of 1:1 (circles) or 1:4 (squares), there were 40% and 50% decreases in Thio-T binding, respectively, suggesting that Sel induces or promotes disassembly of the fibrils. Interestingly, the combination of Sel and DA (triangles) blocks the disaggregating property of Sel and of DA;[50] hence, the decrease in Thio-T binding was similar to that seen upon fibril dilution in the absence of any additive. The LS data shown in Fig. 5b confirm the results of Thio-T binding. Also, since these LS measurements were performed in the absence of added Thio-T, we can rule out that the results observed in Fig. 5a are not due to the competition of Thio-T with Sel or DA for the same binding site on the fibrils.

Evaluating the cytotoxic effect of aggregates formed in the presence of Sel and Sel DA using cultured primary mesencephalic neurons

In a previous study, we demonstrated that although aggregates of α-syn are intracellular in PD, their addition to primary cultures of mesencephalic (dopaminergic) neurons proved to be toxic to these cells.[45] Here we used the same approach to ask if differently aged aggregates formed in the absence or in the presence of Sel would be toxic (see the scheme in Fig. 6c). Toxicity was evaluated by synaptophysin labeling and the formation of pyknotic nuclei, an indicator of apoptosis. Figure 6a and b show images of synaptophysin-labeled neurons from the midbrain of a 14-day-old mouse (E14) to which A30P aggregates of different ages (1, 3, 4, and 5 days old) grown in the absence (Fig. 6a) or in the presence (Fig. 6b) of Sel were added. Figure 6d shows quantification of cell viability by the formation of pyknotic nuclei stained by 4′,6-diamidino-2-phenylindole (DAPI). Interestingly, while the aggregate species formed during the nucleation phase

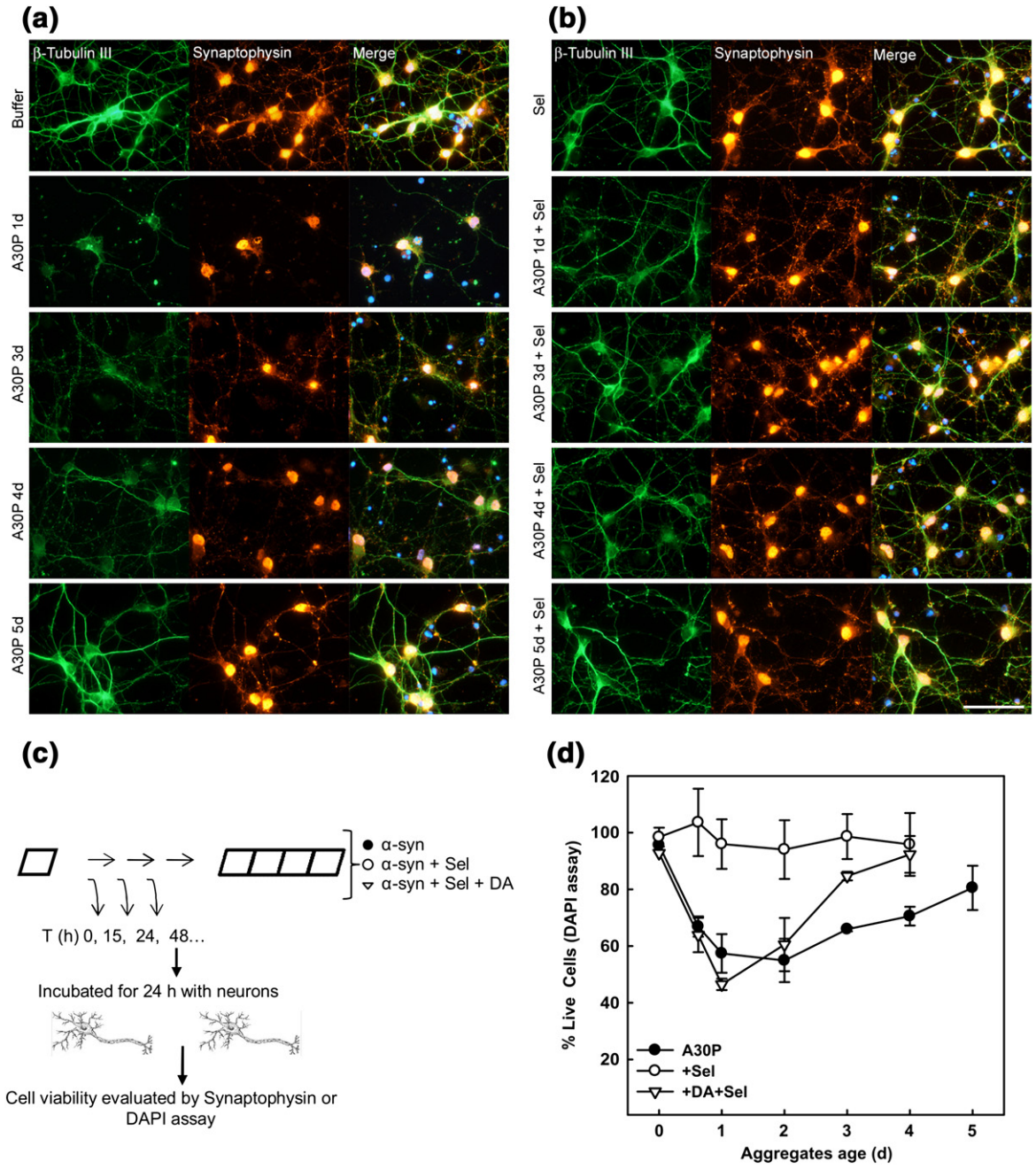

Fig. 6. Aggregates formed in the presence of Sel or DA+Sel display a different toxicity to mesencephalic neurons in culture. (a) Mesencephalic neurons from a 14-day-old embryonic (E14) mouse were maintained for 10 days in culture then treated with 10 μM aggregates grown in the absence (a) or in the presence (b) of 200 μM Sel. Cells were labeled with β-tubulin III (green), synaptophysin (red), and DAPI (blue). (c) Schematic representation of the experimental setup utilized to construct this figure. (d) Percentage of viable cells as measured by nuclear fragmentation (DAPI) after the addition of 10 μM A30P aggregates grown in the absence of Sel and DA (filled circles), in the presence of 200 μM Sel (hollow circles), or in the presence of 140 μM DA + 200 μM Sel (hollow triangles). The ages of the aggregates are displayed in the abscissa. Bars represent the mean ± SD for three independent experiments performed in triplicate.

in the absence of Sel (15 h, 1 day, and 2 days old) were progressively more toxic to mesencephalic neurons (Fig. 6d, filled circles), the aggregates formed during this period of time in the presence of Sel were innocuous to these cells (hollow circles). In the control sample, as aggregates age, their toxicity decreases (filled circles), consistent with the hypothesis of 'nontoxic fibrils.' The images in Fig. 6a and b clearly show the toxic effect of the aggregates formed for up to 4 days in the absence of

Sel (Fig. 6a) in comparison to the toxic effect of the aggregates formed in its presence (Fig. 6b), while the images of the cells treated with 5-day-old aggregates show a similar amount of neurons.

Our next step was to investigate the toxicity of the aggregates formed in the presence of DA Sel to primary mesencephalic neurons using DAPI. Although not presented here, it has been shown previously that protofibrils formed in the presence of DA are toxic to cells in culture.[45,51] As seen in Fig. 6d (inverted triangles), the toxicity of the aggregate species formed in the presence of DA Sel presented a profile similar to that displayed by the control sample (filled circles), with the particularity that their toxicity decreases earlier. These results are consistent with the aggregation profile displayed in Fig. 3a (triangles). In the presence of DA Sel, the lag phase of the aggregation reaction persisted up to ~2d. At this time frame, a mixture of small annular and heterogeneous aggregates is formed, and it resembles those formed in the control sample (compare Figs. 2a and 3d). These species presented the highest toxicity (Fig. 6d). As soon as fibrils are formed due to the counteracting effect of Sel on DA-induced fibril inhibition, Thio-T binding increases and toxicity decreases.

Discussion

Sel as a therapy in PD

Recently, Pålhagen et al. conducted a long-term study demonstrating that Sel delays the progression of the signs and symptoms of PD.[20] Sel significantly delayed the initiation of levodopa therapy; after a 5-year study, the mean dose of levodopa was 19% higher in placebo-treated PD patients than in Sel-treated PD patients. These results confirm the benefits of treating PD patients with Sel, a safe and well-tolerated drug. In spite of all its clinical benefits, the mechanism underlying Sel neuroprotection remains obscure, although several hypotheses have been proposed.[21,25,52,53] Apart from its selective inhibition of MAO-B and its anti-oxidant properties, Sel prevents apoptosis in dopaminergic neurons in MPTP-induced PD animal models.[54] This anti-apoptotic effect, which is also observed with other propargylamines, has not been ascribed to MAO-B inhibition.[55] It has been suggested that propargylamines may rescue degenerating dopaminergic neurons by inhibiting cell death signal transduction initiated from mitochondrial permeability transition, which is a sudden increase in inner-membrane permeability to proteins with a molecular mass below 1500 Da, and may induce a decline in mitochondrial membrane potential. For example, rasagiline prevents mitochondrial permeability transition directly and indirectly through induction of the anti-apoptotic protein Bcl-2 and the glial-cell-line-derived neurotrophic factor.[56] Long-term administration of propargylamines to rats increased the activities of the anti-oxidation enzymes superoxide dismutase and catalase in regions of the brain containing dopaminergic neurons.[57,58]

Effects of Sel on protein aggregation: The case of α-syn

Recently, Ono et al. studied the effects of several anti-parkinsonian agents on the *in vitro* aggregation of amyloid β,[59] the peptide involved in Alzheimer's dementia. Among these agents were DA and Sel, which effectively inhibited amyloid β fibril formation and destabilized preformed fibrils by an unknown mechanism. More recently, the same group evaluated the effects of these agents on α-syn aggregation using the WT protein as model.[27] They showed that Sel disassembles preformed α-syn fibrils in addition to inhibiting fibrillation.

Here, we conducted a series of biophysical and cellular studies that aimed to elucidate the molecular mechanism underlying the effects of Sel on α-syn aggregation and on the structural properties and stability of α-syn aggregates. We have shown that Sel also inhibits the aggregation of A30P, a variant of α-syn involved in a familial form of PD. Moreover, we were able to pinpoint the nucleation phase as the step in the A30P aggregation process at which Sel acts preferentially (Fig. 1b–d). Experiments with the WT protein (Fig. 1f) also suggested that this phase was the target for Sel intervention. This conclusion was based on the observation that Sel increases the lag phase from 15 h to 1.5–5 days (Fig. 1b), as well as on its inefficacy in inhibiting α-syn aggregation when added after nuclei formation (Fig. 1c) or in combination with preformed seeds, which act as nuclei for fibril extension (Fig. 1d and f).

The importance of nucleation events in amyloid formation was revisited recently by Knowles et al.[60] In this study, they presented an analytical treatment showing that the secondary event of nucleation is a determinant for amyloid growth in the cases studied. This secondary event of nucleation comprises the formation of additional nuclei coming from fibril fragmentation. At this moment, we do not have a robust set of data for α-syn (spanning protein concentrations at 2 orders of magnitude) to make this analysis.

NMR data did not reveal any specific residue to which Sel would bind, suggesting that either Sel does not interact with monomeric unfolded α-syn or this interaction was not revealed by NMR experiments performed here (Fig. 4). Thus, we propose that Sel does not bind specifically to any residue in α-syn and probably exerts its effect by binding to an early intermediate species that is present in the aggregation pathway of α-syn, which forms before

nucleus formation, since Sel effects are not as prominent anymore in the presence of preformed seeds (Fig. 1c, d, and f). This Sel-bound intermediates are then converted into aberrant aggregates as seen by EM (Fig. 2a), but they are not off-pathway, since their conversion into fibrils is only delayed but not totally impeded (Fig. 1b). This proposition is supported by the data obtained with Sup35 and TTR, in which Sel was able to inhibit the aggregation of the former, which depends on the formation of a nuclei (Supplementary Fig. 2), but was ineffective in inhibiting the aggregation of the latter, which depends on tetramer dissociation and monomer partial unfolding. With the data presented here, it is not possible to propose a mechanism through which Sel binding would lead to the formation of these aberrant aggregates, but specific protein–protein interactions are responsible for nuclei formation, and they might be compromised by Sel binding to a crucial intermediate species that is present in the pathway of α-syn fibrillation. Sel binding probably bypasses the formation of toxic prefibrillar species but not of the fibrils *per se*, which is interesting for PD therapy, as discussed in the text. SDS susceptibility experiments (Fig. 2d and e) also revealed that although the morphology of the prefibrillar aggregates formed in the presence of Sel is different from the morphology of those formed in its absence, their susceptibilities to SDS solubilization were quite similar (Fig. 2d and e), suggesting that they are somehow structurally related but unrelated in terms of activity (Fig. 6d).

Very recently, Di Giovanni et al. showed that several catechol-containing compounds, which inhibited α-syn aggregation and seeding capacity, also did not bind to monomeric α-syn as probed by NMR.[61] In contrast, the polyphenol epigallocatechin gallate (EGCG), which also inhibited the aggregation of α-syn (leading to the formation of off-pathway oligomers), interacts with the backbone of monomeric α-syn.[62] Lendel et al. showed that Congo red and lacmoid interact with the N-terminal and central regions of α-syn, inhibiting its aggregation.[47] In conclusion, these various studies suggest that different compounds can function as potent α-syn aggregation inhibitors either by interacting directly with the monomeric protein or by interacting directly with an intermediate species that is present in the pathway to fibril formation.

Sel redirects aggregation to the formation of nontoxic oligomers

Coincubation of α-syn with 200 μM Sel for 4–5 days led to the formation of Thio-T-negative amorphous aggregates and larger annular-like structures (Fig. 2). Annular-ring-like aggregates ranging in diameter from 15 to 20 nm have been observed previously in aggregated α-syn solutions[63] and constitute the major species present when α-syn aggregates in the presence of DA.[64,65] The annular structures formed in the presence of Sel were much larger in diameter, ranging from 40 to 100 nm (Fig. 2a). Thus, it is possible that the association of Sel and α-syn impedes the formation of a compact annular structure, resulting in these aberrant rings, which were probed to be nontoxic to cultured mesencephalic neurons (Fig. 6b and d). Thio-T-positive fibrils are formed in the presence of Sel over time (Figs. 1b and d and 2c); amyloid fibrils are observed by EM imaging amidst the presence of a massive population of amorphous aggregates (Fig. 2). Unfortunately, we cannot distinguish now whether these aberrant annular structures evolve into fibrils over time or if other species derived from them serve as raw materials for fibril formation. It is possible that these structures represent off-pathway aggregates that reenter the pathway upon depletion of monomers. In this case, in doing so, they delay aggregation.

The toxicity of the amorphous aggregates formed in the presence of Sel was assessed using cultured mesencephalic neurons and compared to that formed during the aggregation of A30P alone (Fig. 6). In the absence of Sel, the intermediate species formed are extremely toxic, while the amorphous aggregates formed in the presence of Sel are innocuous to the neurons in culture. Recently, Ehrnhoefer *et al.* conducted an elegant study showing that aggregation of α-syn could be effectively inhibited by the polyphenol EGCG.[62] In the presence of EGCG, α-syn formed spherical off-pathway oligomers that were nontoxic to cells in culture, suggesting that small molecules can remodel and/or redirect the aggregation process of amyloidogenic proteins, resulting in the formation of innocuous species. In our case, Sel also led to the formation of nontoxic aggregates and mature fibrils, which are also nontoxic (Fig. 6b and d). However, as mentioned previously, further studies are required to determine whether these aggregates are on-pathway or off-pathway.

The counteracting effect of Sel on DA-induced protofibril formation

In the present study, the novel effect of DA Sel combination on A30P fibril formation was evaluated. This approach is relevant because it mimics what happens when Sel is administered to PD patients in combination with L-dopa, at least in terms of α-syn aggregation. As mentioned previously, several groups have shown that by-products of DA and L-dopa oxidation inhibit α-syn fibril formation, leading to the accumulation of small, spherical, and annular aggregates, which are also called protofibrils. Protofibrils are known to be very toxic to cells in culture.[66,67] We show here that inhibition of A30P

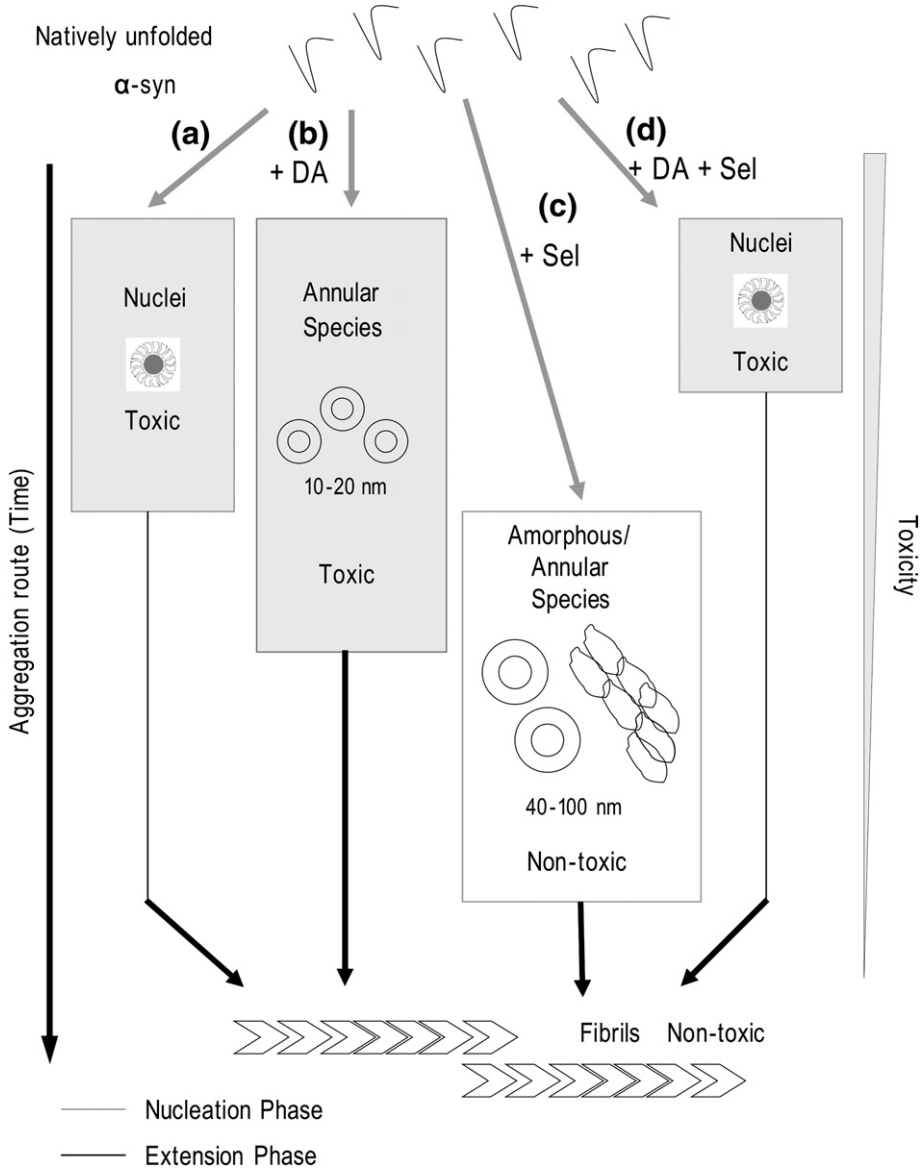

Fig. 7. Proposed model for Sel action on α-syn fibrillogenesis. α-Syn is a natively unfolded protein. (a) Under aggregating conditions, the protein undergoes aggregation through the formation of toxic nuclei that act as seeds for fibrillation. (b) In the presence of DA, fibrillation is inhibited and annular, and toxic species are formed. (c) In the presence of Sel, nucleation is retarded, giving rise to the appearance of amorphous and larger annular aggregates, which are nontoxic to neurons in culture. (d) In the presence of both Sel DA, fibril formation is restored to some extent. The early prefibrillar aggregate species formed in the presence of Sel DA were shown to be toxic to mesencephalic neurons in culture. Their toxicity diminishes as they age, but earlier than that of their age-matched counterparts.

fibril formation by DA is counteracted by Sel, leading to the formation of some mature fibrils (Fig. 3). This result *per se* points to the potential benefit of a combined therapy in PD disease, since mature fibrils are now believed to be less toxic than small aggregates. The precise mechanism behind the counteracting effect of Sel on DA-induced protofibril formation is not known at the present moment. Possible explanations would be the coaggregation of the two compounds, which would prevent DA from exerting its effect, or a direct effect of Sel on the oxidation of DA, which would block the formation of the oxidized active species of DA. The results presented in Supplementary Fig. 3 seem to exclude these possibilities. It has been proposed that DA exerts its effect by forming covalent adducts between the orthoquinone derivative of DA and α-syn,[44] which causes the accumulation of covalently modified protofibrils (annular aggregates) that are unable to fibrillate. As shown here by NMR, Sel does not

specifically bind to soluble α-syn (Fig. 4), but aberrant annular structures are formed in its presence. Therefore, both DA and Sel favor the formation of annular aggregates; those formed in the presence of the former are smaller, off-pathway, and toxic, while those formed in the presence of the latter are larger, on-pathway, and nontoxic to cell lines in culture. When aggregation is performed in the presence of DA and Sel, some amyloid fibrils appear after 6 days under aggregating conditions (Fig. 3d), but some annular aggregates still persist. Thus, it is possible that the reminiscent annular aggregates are those formed by the DA/α-syn adduct, while the fibrils observed are formed from the soluble α-syn that evades this interaction, probably caused by the presence of Sel, which favors annular on-pathway aggregates. Interestingly, the early aggregates formed in the presence of Sel DA were shown to be as toxic as the aggregates formed in the absence of any addition; however, as soon as aggregation proceeds and fibrils are formed, toxicity decreases, but only when DA and Sel are present. This result is also very interesting because the annular aggregates formed in the presence of DA (early and late) are very toxic to cells in culture, as previously shown.[44,66,68]

Conclusions and Implications for PD

A schematic depiction summarizing the main findings of this study is presented in Fig. 7. Natively unfolded α-syn initially forms small nuclei that seed aggregation (nucleation phase; pathway A). These nuclei, which are toxic, are extended by the incorporation of monomers or other species to form mature amyloid fibrils (extension phase). In the presence of DA (pathway B), fibril formation is drastically inhibited, leading to the accumulation of annular toxic aggregates, which could explain the selective cell loss in PD. In the presence of Sel (pathway C), a heterogeneous population of aggregates, mostly composed of amorphous and aberrant large annular structures, is formed. These aggregates, which appear to be less toxic to mesencephalic neurons in culture, delay fibril formation, thus expanding the nucleation phase. However, over time, these aggregates evolve into fibrils by possibly serving as a source of monomers or by becoming amyloid fibrils themselves. In the presence of Sel DA (pathway D), annular and heterogeneous oligomers are formed during the nucleation phase, but some fibrils are observed even though DA inhibits fibril formation. These early aggregates formed in the presence of DA Sel were shown to be toxic to the cells, while the late aggregates were not. Although Sel displays multiple effects when taken by PD patients, the data presented herein disclose a novel mechanism of action (i.e., its effect on α-syn aggregation and fibril formation) that has implications for PD therapy.

In dopaminergic neurons, the presence of DA would lead to the formation of protofibrils, which have been shown to be more toxic to neurons than the mature fibrils. While DA favors the initial steps of fibril formation leading to the accumulation of toxic protofibrils, Sel drives fibril formation in the presence of DA but inhibits fibrillization in the absence of DA. In addition, Sel was able to partially counteract the fibril-disassembling properties of DA (Fig. 5), which can lead to the generation of smaller toxic species. Together, these findings suggest that Sel could act as a detoxifying agent by removing toxic protofibrils via enhancement of their conversion into amyloid fibrils, thus sparing the dopaminergic neurons from the toxic effects of these aggregates. These findings suggest that administration of Sel, in combination with DA, would be beneficial to PD patients by favoring fibril formation. In nondopaminergic neurons, Sel slows the fibrillation process of α-syn, probably by forming large amorphous nontoxic aggregates that evolve into fibrils over time.

Taken together, the data presented here provide new insights into the beneficial mechanism that operates when Sel and L-dopa are administered to patients with parkinsonism. Further *in vivo* studies and analysis of clinical data are necessary to test this hypothesis. To our knowledge, this is the first report in which the combined effect of Sel and DA on the *in vitro* aggregation of the α-syn A30P variant was evaluated, with possible correlations to their use in PD treatment.

Materials and Methods

α-Syn fibrillogenesis

Recombinant α-syn (A30P or WT) was expressed and purified as previously described.[29] Solutions of 140 μM A30P or WT in buffer A [10 mM Tris, 100 mM NaCl, and 0.05% sodium azide (pH 7.4)] were incubated at 37 °C, with shaking at 185 rpm, to allow fibril formation. For cell viability assays, the samples were incubated in buffer A without sodium azide and filtered in a sterile 0.22-μm filter. Fibrillogenesis was monitored by measurement of the absorbance of the solution at 330 nm, as well as by Thio-T binding, until a steady state had been reached. Aggregation in the presence of DA was performed as described by Conway *et al.*[44] and Li *et al.*[50] Briefly, 140 μM A30P was incubated in the presence of an equimolar concentration of DA in buffer A and allowed to aggregate as described above. To test the effect of Sel (*R*(−)-deprenyl; Sigma Chemical Co.) and/or DA (Sigma Chemical Co.) on α-syn aggregation, we incubated 140 μM A30P in the presence of each of these compounds at the concentrations stated in the legend to each experiment.

Aggregation of Sup35 and TTR

Soluble WT Sup35 was prepared as described previously by Serio et al.[69] Concentrated Sup35 was diluted at least 200-fold into phosphate buffer [5 mM potassium phosphate and 150 mM NaCl (pH 7.4)] to a concentration of 0.5 μM. Aggregation was performed with microstir bars at 25 °C under constant agitation (60 rpm) using 20 μM Thio-T binding as an indicator of fibril formation. Sel was added to the aggregation solutions as stated in Supplementary Fig. 2. For TTR aggregation, 3.5 μM TTR was incubated at 37 °C for 72 h in 50 mM sodium acetate, 100 mM KCl, and 0.05% NaN_3 (pH 4.4) in the absence or in the presence of 5 or 14 μM Sel. The aggregation was measured by the turbidity at 330 nm.

DA oxidation

To assay the oxidation of DA in the absence or in the presence of Sel, we incubated the compounds at 37 °C and measured the optical density at 386 nm as described by Klegeris *et al.*[46]

Thio-T binding

The extent of aggregation was evaluated by Thio-T binding. In the case of α-syn, suspensions containing the aggregated proteins were diluted to 1 μM and mixed with 20 μM Thio-T (Sigma Chemical Co.) prepared in 50 mM glycine (pH 8.5) in a total volume of 600 μl. Thio-T binding was evaluated by measuring the increase in fluorescence spectral area and the intensity at 482 nm after excitation of the sample at 450 nm and collection of emission spectra from 465 to 570 nm. The results of Thio-T binding are expressed as the means of at least two separate experiments, and the data were fitted using a sigmoidal regression of three parameters.

Circular dichroism

CD spectra were recorded in a Jasco-715 spectropolarimeter (Jasco, Tokyo, Japan). Buffer A (without NaN_3) was used as baseline and subtracted from the protein spectra. The protein was diluted to a final concentration of 70 μM in buffer A. Following its dilution, the solution was transferred to a 2-mm quartz cuvette, and CD spectra were recorded from 195 to 260 nm at 25 °C. Secondary structural content was calculated under each condition with the algorithm Contin or k2d[70] using the reference set SP175‡.[71–73]

SDS-PAGE analysis of the aggregates

A30P (140 μM) was incubated in the absence or in the presence of 200 μM Sel under aggregating conditions. After the indicated time periods, 200-μl aliquots were collected, lyophilized, and resuspended in 50 μl of SDS sample buffer. Twenty microliters of each sample was loaded in 15% SDS-PAGE, and the bands were visualized with silver staining.

‡ http://dichroweb.cryst.bbk.ac.uk

NMR experiments

Samples for NMR experiments were prepared by diluting lyophilized ^{15}N-labeled protein directly in sample buffer [10 mM phosphate buffer, 100 mM NaCl (pH 7.4), and 10% D_2O] at a final concentration of 350 μM in the absence or in the presence of Sel. Large aggregates were removed by centrifugation at 11,000*g* for 10 min. All NMR samples were prepared in an ice bath to minimize protein aggregation. All experiments were performed at the ^1H NMR frequency of 800.4 MHz using a Bruker DRX 800-MHz narrow bore. The spectra were acquired at 10 °C. For samples incubated in the presence of Sel, the compound was added to a solution containing an uniformly ^{15}N α-syn molar ratio of 1:1; 1:2, or 1:5. Spectra were processed with topspin and analyzed using the ^{15}N and ^1H chemical shift assignments previously established by Eliezer *et al.*[48]

Disassembly of A30P fibrils induced by Sel, DA, or DA Sel

Solutions containing 140 μM A30P were incubated for 15 days under aggregating conditions. Then, the fibrils were centrifuged and resuspended in buffer A. After measuring the concentration of protein (OD_{280}), we diluted the fibrils to 10 μM in buffer A with either DA (10 μM), Sel (10 or 40 μM), or a combination of DA Sel (10 40 μM) in a final volume of 1500 μl and gently stirred them at 37 °C. To evaluate the extent of A30P fibril disassembly promoted by these compounds, we followed Thio-T binding with respect to time, as stated above. In the experiments where LS was measured, the fibrils were incubated with the compounds in the absence of Thio-T. All results are expressed as the mean of at least three separate experiments. The LS data were evaluated statistically with analysis of variance (Tukey's multiple comparison test) using the software Prism (GraphPad Software, Inc., San Diego, CA).

Transmission EM

Samples were adhered to a carbon-coated grid, blotted to remove excess material, and stained for 2 min with a 2% solution of uranyl acetate prepared in water. Images were digitally collected with a Jeol 1200 electron microscope (Jeol Ltd., Tokyo, Japan) operating at 60 kV.

Primary neuron cultures

Neurons from the midbrain of 14-day-old Swiss mice (E14) were prepared as previously described.[74] All animals were kept under standard laboratory conditions in accordance with National Institutes of Health guidelines. Mice anesthetized by hypothermia were decapitated; their brain structures were removed, and their meninges were carefully stripped off. Dissociated cells were plated on coverslips coated with polyornithine (1.5 mg/ml; Sigma Chemical Co.) in serum-free neurobasal medium

supplemented with B27 (Invitrogen, Carlsbad, CA). For immunocytochemistry assays, cells were plated on poly-ornithine-treated glass coverslips. The cultures were incubated at 37 °C in a humidified 5% CO_2 and 95% air chamber for 10 days.

Immunocytochemistry

Immunocytochemistry was performed as previously described by Romão *et al.*[74] Briefly, cultured cells were fixed with 4% paraformaldehyde for 20 min and permeabilized with 0.2% Triton X-100 for 5 min at room temperature. After permeabilization, the cells were blocked with 10% normal goat serum (Vector Laboratories, Inc., Burlingame, CA) in phosphate-buffered saline (PBS) (blocking solution) for 1 h, followed by an overnight incubation with specified primary antibodies diluted in blocking solution at room temperature. The primary antibodies were polyclonal anti-human β-tubulin III (1:800; Covance) and monoclonal anti-synaptophysin (1:200; Chemicon International). Monoclonal anti-tyrosine hydroxylase antibody (1:100; Sigma Chemical Co.) was used to quantify dopaminergic neurons and accounted for 95% of the cells in culture. After the incubation of the primary antibodies, the cells were extensively washed with PBS/10% normal goat serum and incubated with secondary antibodies for 1 h at room temperature. Secondary antibodies were conjugated with fluorescein isothiocyanate or Alexa (sheep anti-mouse; 1:400; Sigma Chemical Co.). Nuclear DNA was counterstained with 0.1 μg/ml 4,6-diamidino-2-phenylindole (DAPI; Sigma Chemical Co.) for 5 min at room temperature, washed with PBS, and mounted on fluorescence medium. Negative control samples were performed by omitting the primary antibodies during staining. In all cases, no reactivity was observed when the primary antibodies were omitted.

Neurotoxicity assays

After 10 days of incubation, neuron cultures were treated with A30P aggregates of different ages (15 h, 1 day, 2 days, 3 days, and 4 days). The toxic effects of these aggregates (at a concentration of 10 μM) were evaluated after 24 h of incubation in neuronal cell cultures. Toxicity was evaluated by analyzing nuclear fragmentation with DAPI, as described above. Randomly chosen fields were examined and counted in a Nikon Eclipse TE300 microscope (Nikon, Kanagawa, Japan). Five different fields (~200 cells/field) were examined per well, and three cultures were used under each experimental condition. Buffer was used as control.

Supplementary materials related to this article can be found online at doi:10.1016/j.jmb.2010.10.027

Acknowledgements

We are grateful to Emerson R. Gonçalves for competent technical assistance, Leonardo C. Palmieri and Prof. Ana Paula Valente for help with NMR experiments, and Prof. Kildare Miranda and Laboratório de Ultraestrutura Celular Hertha Meyer for assistance with the transmission electron microscope. This work was supported by grants from Conselho Nacional de Desenvolvimento Científico e Tecnológico, Coordenação de Aperfeicoamento de Pessoal de Nível Superior, and by Fundação de Amparo a Pesquisa no Estado do Rio de Janeiro. This work was also supported by Instituto Nacional de Ciência e Tecnologia em Biologia Estrutural e Bioimagem (Conselho Nacional de Desenvolvimento Científico e Tecnológico/Fundação de Amparo a Pesquisa no Estado do Rio de Janeiro).

References

1. Tanner, C. M. (1992). Epidemiology of Parkinson's disease. *Neurol. Clin.* **10**, 317–329.
2. Forno, L. S. (1996). Neuropathology of Parkinson's disease. *J. Neuropathol. Exp. Neurol.* **55**, 259–272.
3. Baba, M., Nakajo, S., Tu, P. H., Tomita, T., Nakaya, K., Lee, V. M. *et al.* (1998). Aggregation of alpha-synuclein in Lewy bodies of sporadic Parkinson's disease and dementia with Lewy bodies. *Am. J. Pathol.* **152**, 879–884.
4. Goedert, M. (2001). Alpha-synuclein and neurodegenerative diseases. *Nat. Rev. Neurosci.* **2**, 492–501.
5. Uversky, V. N. (2008). Alpha-synuclein misfolding and neurodegenerative diseases. *Curr. Protein Pept. Sci.* **9**, 507–540.
6. Krüger, R., Kuhn, W., Müller, T., Woitalla, D., Graeber, M., Kösel, S. *et al.* (1998). Ala30Pro mutation in the gene encoding alpha-synuclein in Parkinson's disease. *Nat. Genet.* **18**, 106–108.
7. Conway, K. A., Lee, S. J., Rochet, J. C., Ding, T. T., Williamson, R. E., Lansbury, P. T. *et al.* (2000). Acceleration of oligomerization, not fibrillization, is a shared property of both alpha-synuclein mutations linked to early-onset Parkinson's disease: implications for pathogenesis and therapy. *Proc. Natl Acad. Sci. USA*, **97**, 571–576.
8. Singleton, A. B., Farrer, M., Johnson, J., Singleton, A., Hague, S., Kachergus, J. *et al.* (2003). Alpha-synuclein locus triplication causes Parkinson's disease. *Science*, **302**, 841.
9. Maraganore, D. M., Wilkes, K., Lesnick, T. G., Strain, K. J., de Andrade, M., Rocca, W. A. *et al.* (2004). A limited role for DJ1 in Parkinson disease susceptibility. *Neurology*, **63**, 550–553.
10. Singleton, A., Gwinn-Hardy, K., Sharabi, Y., Li, S., Holmes, C., Dendi, R. *et al.* (2004). Association between cardiac denervation and parkinsonism caused by alpha-synuclein gene triplication. *Brain*, **127**, 768–772.
11. Conway, K. A., Harper, J. D. & Lansbury, P. T. J. (2000). Fibrils formed *in vitro* from alpha-synuclein and two mutant forms linked to Parkinson's disease are typical amyloid. *Biochemistry*, **39**, 2552–2563.
12. Li, J., Uversky, V. N. & Fink, A. L. (2001). Effect of familial Parkinson's disease point mutations A30P and A53T on the structural properties, aggregation, and fibrillation of human alpha-synuclein. *Biochemistry*, **40**, 11604–11613.

13. Fredenburg, R. A., Rospigliosi, C., Meray, R. K., Kessler, J. C., Lashuel, H. A., Eliezer, D. *et al.* (2007). The impact of the E46K mutation on the properties of alpha-synuclein in its monomeric and oligomeric states. *Biochemistry*, **46**, 7107–7118.
14. Elsworth, J. D., Glover, V., Reynolds, G. P., Sandler, M., Lees, A. J., Phuapradit, P. *et al.* (1978). Deprenyl administration in man: a selective monoamine oxidase B inhibitor without the 'cheese effect'. *Psychopharmacology (Berlin)*, **57**, 33–38.
15. Langston, J. W., Ballard, P., Tetrud, J. W. & Irwin, I. (1983). Chronic parkinsonism in humans due to a product of meperidine-analog synthesis. *Science*, **219**, 979–980.
16. Heikkila, R. E., Manzino, L., Cabbat, F. S. & Duvoisin, R. C. (1984). Protection against the dopaminergic neurotoxicity of 1-methyl-4-phenyl-1,2,5,6-tetrahydropyridine by monoamine oxidase inhibitors. *Nature*, **311**, 467–469.
17. Langston, J. W. & Tanner, C. M. (2000). Selegiline and Parkinson's disease: it's déjà vu—again. *Neurology*, **55**, 1770–1771.
18. Jenner, P. & Olanow, C. W. (1996). Oxidative stress and the pathogenesis of Parkinson's disease. *Neurology*, **47**, S161–S170.
19. Przedborski, S., Jackson-Lewis, V., Djaldetti, R., Liberatore, G., Vila, M., Vukosavic, S. & Almer, G. (2000). The parkinsonian toxin MPTP: action and mechanism. *Restor. Neurol. Neurosci.* **16**, 135–142.
20. Pålhagen, S., Heinonen, E., Hägglund, J., Kaugesaar, T., Mäki-Ikola, O. & Palm, R. (2006). Selegiline slows the progression of the symptoms of Parkinson disease. *Neurology*, **66**, 1200–1206.
21. Ebadi, M., Sharma, S., Shavali, S. & El Refaey, H. (2002). Neuroprotective actions of selegiline. *J. Neurosci. Res.* **67**, 285–289.
22. Lees, A. (2005). Alternatives to levodopa in the initial treatment of early Parkinson's disease. *Drugs Aging*, **22**, 731–740.
23. Mytilineou, C., Radcliffe, P., Leonardi, E. K., Werner, P. & Olanow, C. W. (1997). L-Deprenyl protects mesencephalic dopamine neurons from glutamate receptor-mediated toxicity *in vitro*. *J. Neurochem.* **68**, 33–39.
24. Paterson, I. A. & Tatton, W. G. (1998). Antiapoptotic actions of monoamine oxidase B inhibitors. *Adv. Pharmacol.* **42**, 312–315.
25. Maruyama, W., Takahashi, T. & Naoi, M. (1998). (-)-Deprenyl protects human dopaminergic neuroblastoma SH-SY5Y cells from apoptosis induced by peroxynitrite and nitric oxide. *J. Neurochem.* **70**, 2510–2515.
26. Ondo, W. G., Sethi, K. D. & Kricorian, G. (2007). Selegiline orally disintegrating tablets in patients with Parkinson disease and "wearing off" symptoms. *Clin. Neuropharmacol.* **30**, 295–300.
27. Ono, K., Hirohata, M. & Yamada, M. (2007). Anti-fibrillogenic and fibril-destabilizing activities of anti-parkinsonian agents for alpha-synuclein fibrils *in vitro*. *J. Neurosci. Res.* **85**, 1547–1557.
28. Uversky, V. N. & Eliezer, D. (2009). Biophysics of Parkinson's disease: structure and aggregation of alpha-synuclein. *Curr. Protein Pept. Sci.* **10**, 483–499.
29. Conway, K. A., Harper, J. D. & Lansbury, P. T. (1998). Accelerated *in vitro* fibril formation by a mutant alpha-synuclein linked to early-onset Parkinson disease. *Nat. Med.* **4**, 1318–1320.
30. Narhi, L., Wood, S. J., Steavenson, S., Jiang, Y., Wu, G. M., Anafi, D. *et al.* (1999). Both familial Parkinson's disease mutations accelerate alpha-synuclein aggregation. *J. Biol. Chem.* **274**, 9843–9846.
31. Zhou, W., Hurlbert, M. S., Schaack, J., Prasad, K. N. & Freed, C. R. (2000). Overexpression of human alpha-synuclein causes dopamine neuron death in rat primary culture and immortalized mesencephalon-derived cells. *Brain Res.* **866**, 33–43.
32. Lashuel, H. A., Petre, B. M., Wall, J., Simon, M., Nowak, R. J., Walz, T. & Lansbury, P. T. (2002). Alpha-synuclein, especially the Parkinson's disease-associated mutants, forms pore-like annular and tubular protofibrils. *J. Mol. Biol.* **322**, 1089–1102.
33. Paleologou, K. E., Schmid, A. W., Rospigliosi, C. C., Kim, H., Lamberto, G. R., Fredenburg, R. A. *et al.* (2008). Phosphorylation at Ser-129 but not the phosphomimics S129E/D inhibits the fibrillation of alpha-synuclein. *J. Biol. Chem.* **283**, 16895–16905.
34. Yagi, H., Kusaka, E., Hongo, K., Mizobata, T. & Kawata, Y. (2005). Amyloid fibril formation of alpha-synuclein is accelerated by preformed amyloid seeds of other proteins: implications for the mechanism of transmissible conformational diseases. *J. Biol. Chem.* **280**, 38609–38616.
35. Bussell, R. J. & Eliezer, D. (2001). Residual structure and dynamics in Parkinson's disease-associated mutants of alpha-synuclein. *J. Biol. Chem.* **276**, 45996–46003.
36. Jarrett, J. T. & Lansbury, P. T. J. (1993). Seeding "one-dimensional crystallization" of amyloid: a pathogenic mechanism in Alzheimer's disease and scrapie? *Cell*, **73**, 1055–1058.
37. Wood, S. J., Wypych, J., Steavenson, S., Louis, J. C., Citron, M. & Biere, A. L. (1999). Alpha-synuclein fibrillogenesis is nucleation-dependent. Implications for the pathogenesis of Parkinson's disease. *J. Biol. Chem.* **274**, 19509–19512.
38. Pellarin, R. & Caflisch, A. (2006). Interpreting the aggregation kinetics of amyloid peptides. *J. Mol. Biol.* **360**, 882–892.
39. Cerdà-Costa, N., Esteras-Chopo, A., Avilés, F. X., Serrano, L. & Villegas, V. (2007). Early kinetics of amyloid fibril formation reveals conformational reorganisation of initial aggregates. *J. Mol. Biol.* **366**, 1351–1363.
40. Chiti, F., Webster, P., Taddei, N., Clark, A., Stefani, M., Ramponi, G. & Dobson, C. M. (1999). Designing conditions for *in vitro* formation of amyloid protofilaments and fibrils. *Proc. Natl Acad. Sci. USA*, **96**, 3590–3594.
41. Hurshman, A. R., White, J. T., Powers, E. T. & Kelly, J. W. (2004). Transthyretin aggregation under partially denaturing conditions is a downhill polymerization. *Biochemistry*, **43**, 7365–7381.
42. Cappai, R., Leck, S., Tew, D. J., Williamson, N. A., Smith, D. P., Galatis, D. *et al.* (2005). Dopamine promotes alpha-synuclein aggregation into SDS-resistant soluble oligomers via a distinct folding pathway. *FASEB J.* **19**, 1377–1379.
43. Pham, C. L. L., Leong, S. L., Ali, F. E., Kenche, V. B., Hill, A. F., Gras, S. L. *et al.* (2009). Dopamine and the

dopamine oxidation product 5,6-dihydroxylindole promote distinct on-pathway and off-pathway aggregation of alpha-synuclein in a pH-dependent manner. *J. Mol. Biol.* **387**, 771–785.
44. Conway, K. A., Rochet, J. C., Bieganski, R. M. & Lansbury, P. T. J. (2001). Kinetic stabilization of the alpha-synuclein protofibril by a dopamine–alpha-synuclein adduct. *Science*, **294**, 1346–1349.
45. Follmer, C., Romão, L., Einsiedler, C. M., Porto, T. C. R., Lara, F. A., Moncores, M. *et al.* (2007). Dopamine affects the stability, hydration, and packing of protofibrils and fibrils of the wild type and variants of alpha-synuclein. *Biochemistry*, **46**, 472–482.
46. Klegeris, A., Korkina, L. G. & Greenfield, S. A. (1995). Autoxidation of dopamine: a comparison of luminescent and spectrophotometric detection in basic solutions. *Free Radical Biol. Med.* **18**, 215–222.
47. Lendel, C., Bertoncini, C. W., Cremades, N., Waudby, C. A., Vendruscolo, M. & Dobson, C. M. (2009). On the mechanism of nonspecific inhibitors of protein aggregation: dissecting the interactions of alpha-synuclein with Congo red and lacmoid. *Biochemistry*, **48**, 8322–8334.
48. Eliezer, D., Kutluay, E., Bussell, R. J. & Browne, G. (2001). Conformational properties of alpha-synuclein in its free and lipid-associated states. *J. Mol. Biol.* **307**, 1061–1073.
49. Glushka, J., Lee, M., Coffin, S. & Cowburn, D. (1989). ^{15}N chemical shifts of backbone amides in bovine pancreatic trypsin inhibitor and apamin. *J. Am. Chem. Soc.* **111**, 7716–7722.
50. Li, J., Zhu, M., Manning-Bog, A. B., Di Monte, D. A. & Fink, A. L. (2004). Dopamine and L-dopa disaggregate amyloid fibrils: implications for Parkinson's and Alzheimer's disease. *FASEB J.* **18**, 962–964.
51. Li, H., Lin, D., Luo, X., Zhang, F., Ji, L., Du, H. N. *et al.* (2005). Inhibition of alpha-synuclein fibrillization by dopamine analogs via reaction with the amino groups of alpha-synuclein. Implication for dopaminergic neurodegeneration. *FEBS J.* **272**, 3661–3672.
52. Gerlach, M., Youdim, M. B. & Riederer, P. (1996). Pharmacology of selegiline. *Neurology*, **47**, S137–S145.
53. Stocchi, F. & Olanow, C. W. (2003). Neuroprotection in Parkinson's disease: clinical trials.*Ann. Neurol.* **53**, S87–S97; discussion, S97–S99.
54. Tatton, W. G. & Greenwood, C. E. (1991). Rescue of dying neurons: a new action for deprenyl in MPTP parkinsonism. *J. Neurosci. Res.* **30**, 666–672.
55. Naoi, M. & Maruyama, W. (2001). Future of neuroprotection in Parkinson's disease. *Parkinsonism-Relat. Disord.* **8**, 139–145.
56. Weinreb, O., Amit, T., Bar-Am, O. & Youdim, M. B. H. (2010). Rasagiline, a novel anti-parkinsonian monoamine oxidase-B inhibitor with neuroprotective activity. *Prog. Neurobiol.* E-publication ahead of print.
57. Weinreb, O., Bar-Am, O., Amit, T., Chillag-Talmor, O. & Youdim, M. B. H. (2004). Neuroprotection via pro-survival protein kinase C isoforms associated with Bcl-2 family members. *FASEB J.* **18**, 1471–1473.
58. Maruyama, W., Akao, Y., Carrillo, M. C., Kitani, K., Youdium, M. B. H. & Naoi, M. (2002). Neuroprotection by propargylamines in Parkinson's disease: suppression of apoptosis and induction of prosurvival genes. *Neurotoxicol. Teratol.* **24**, 675–682.
59. Ono, K., Hasegawa, K., Naiki, H. & Yamada, M. (2006). Anti-parkinsonian agents have anti-amyloidogenic activity for Alzheimer's beta-amyloid fibrils *in vitro*. *Neurochem. Int.* **48**, 275–285.
60. Knowles, T. P. J., Waudby, C. A., Devlin, G. L., Cohen, S. I. A., Aguzzi, A., Vendruscolo, M. *et al.* (2009). An analytical solution to the kinetics of breakable filament assembly. *Science*, **326**, 1533–1537.
61. Di Giovanni, S., Eleuteri, S., Paleologou, K. E., Yin, G., Zweckstetter, M., Carrupt, P. A. & Lashuel, H. A. (2010). Entacapone and tolcapone, two catechol-*O*-methyltransferase inhibitors (ICOMT), block fibril formation of {alpha}-synuclein and {beta}-amyloid and protect against amyloid-induced toxicity. *J. Biol. Chem.* **285**, 14941–14954.
62. Ehrnhoefer, D. E., Bieschke, J., Boeddrich, A., Herbst, M., Masino, L., Lurz, R. *et al.* (2008). EGCG redirects amyloidogenic polypeptides into unstructured, off-pathway oligomers. *Nat. Struct. Mol. Biol.* **15**, 558–566.
63. Ding, T. T., Lee, S., Rochet, J. & Lansbury, P. T. J. (2002). Annular alpha-synuclein protofibrils are produced when spherical protofibrils are incubated in solution or bound to brain-derived membranes. *Biochemistry*, **41**, 10209–10217.
64. Rochet, J., Outeiro, T. F., Conway, K. A., Ding, T. T., Volles, M. J., Lashuel, H. A. *et al.* (2004). Interactions among alpha-synuclein, dopamine, and biomembranes: some clues for understanding neurodegeneration in Parkinson's disease. *J. Mol. Neurosci.* **23**, 23–34.
65. Norris, E. H., Giasson, B. I., Hodara, R., Xu, S., Trojanowski, J. Q., Ischiropoulos, H. & Lee, V. M. (2005). Reversible inhibition of alpha-synuclein fibrillization by dopaminochrome-mediated conformational alterations. *J. Biol. Chem.* **280**, 21212–21219.
66. Volles, M. J. & Lansbury, P. T. J. (2002). Vesicle permeabilization by protofibrillar alpha-synuclein is sensitive to Parkinson's disease-linked mutations and occurs by a pore-like mechanism. *Biochemistry*, **41**, 4595–4602.
67. Volles, M. J. & Lansbury, P. T. J. (2003). Zeroing in on the pathogenic form of alpha-synuclein and its mechanism of neurotoxicity in Parkinson's disease. *Biochemistry*, **42**, 7871–7878.
68. Lashuel, H. A., Hartley, D., Petre, B. M., Walz, T. & Lansbury, P. T. J. (2002). Neurodegenerative disease: amyloid pores from pathogenic mutations. *Nature*, **418**, 291.
69. Serio, T. R., Cashikar, A. G., Moslehi, J. J., Kowal, A. S. & Lindquist, S. L. (1999). Yeast prion [psi^{+-}] and its determinant, Sup35p. *Methods Enzymol.* **309**, 649–673.
70. Andrade, M. A., Chacón, P., Merelo, J. J. & Morán, F. (1993). Evaluation of secondary structure of proteins from UV circular dichroism spectra using an unsupervised learning neural network. *Protein Eng.* **6**, 383–390.
71. Lees, J. G., Miles, A. J., Wien, F. & Wallace, B. A. (2006). A reference database for circular dichroism spectroscopy covering fold and secondary structure space. *Bioinformatics*, **22**, 1955–1962.

72. Whitmore, L. & Wallace, B. A. (2004). DICHROWEB, an online server for protein secondary structure analyses from circular dichroism spectroscopic data. *Nucleic Acids Res.* **32**, W668–W673.
73. Whitmore, L. & Wallace, B. A. (2008). Protein secondary structure analyses from circular dichroism spectroscopy: methods and reference databases. *Biopolymers*, **89**, 392–400.
74. Romão, L. F., Sousa, V. D. O., Neto, V. M. & Gomes, F. C. A. (2008). Glutamate activates GFAP gene promoter from cultured astrocytes through TGF-beta1 pathways. *J. Neurochem.* **106**, 746–756.